Supporting Information

Keggin-Type Polyoxometalate-Containing Metal-Organic Hybrids as Friction Materials for Triboelectric Nanogenerators

Ying-Ying Zhang,[‡a] Mingjun Hu,[‡a] Zhichao Shao,[a] Chao Huang,[*a] Qi Qin[*a] and Liwei Mi[*a]

Table of Contents

1. Experimental Procedures

1.1 Materials

Zinc nitrate hexahydrate ($Zn(NO_3)_2 \cdot 6H_2O$), Copper(II) nitrate trihydrate ($Cu(NO_3)_2 \cdot 3H_2O$), N,N-Dimethylacetamide (DMA), Acetone (CH_3COCH_3), Nitric acid (HNO_3) were purchased from China Pharmaceutical Group Chemical Reagents Co., Ltd. Sodium tungstate dehydrate ($Na_2WO_4 \cdot 2H_2O$) were purchased from Aladdin. 4,4'-Bipyridine (4,4'-bpy) and 2,4,6-Tri(4-pyridyl)-1,3,5-triazine (TPT) were purchased from J&K Chemicals. Poly(vinylidene fluoride) (PVDF, average Mw ~534,000 by GPC, powder) were purchased from Sigma-Aldrich. The above chemicals were purchased and used without further purification. The polyoxometalate ($(H_2NMe_2)_5H[ZnW_{12}O_{40}] \cdot 3.5H_2O$) was prepared under hydrothermal conditions according to the reported procedure.[1]

1.2 Synthesis of 1

A mixture of $Zn(NO_3)_2 \cdot 6H_2O$ (0.082 g, 0.276 mmol), 4,4'-bpy (0.043g 0.276 mmol), $Na_2WO_4 \cdot 2H_2O$ (0.273 g, 0.828 mmol), was dissolved in deionized (DI) water (16 mL) and stirred at room temperature for 30 minutes. The pH value of the mixture was adjusted to 4.8 by HNO_3. And then, the mixture was placed in the 30 mL Teflon lined stainless steel, kept at 140 °C for 3.5 days, and then cooled to room temperature at a cooling rate of 5 °C h^{-1}. Colorless bulk single crystals are filtered, washed with deionized water and dried at room temperature (48.39 % yield based on W). Elemental analysis calcd (%) for $C_{40}H_{44}N_8O_{44}W_{12}Zn_2$: C, 13.06; H, 1.21; N, 3.05; found C, 12.98; H, 1.25; N, 2.99. IR (KBr pellets, ν/cm^{-1}): 3420 (w), 3074 (w), 2360 (w), 1616 (w), 1559 (w), 1489 (w), 1410 (w), 1206 (w), 1076 (w), 936 (s), 880 (s), 753 (s), 566 (m), 452 (m).

1.3 Synthesis of 2

A mixture of $Zn(NO_3)_2 \cdot 6H_2O$ (0.041 g, 0.138 mmol), $Cu(NO_3)_2 \cdot 3H_2O$ (0.067 g, 0.276 mmol), TPT (0.086 g 0.276 mmol), $Na_2WO_4 \cdot 2H_2O$ (0.273 g, 0.828 mmol), was dissolved in deionized (DI) water (10 mL) and stirred at room temperature for 30 minutes. The pH value of the mixture was adjusted to 4.8 by HNO3.

And then, the mixture was placed in the 30 mL Teflon lined stainless steel, kept at 140 °C for 3.5 days, and then cooled to room temperature at a cooling rate of 5 °C h^{-1}. Green bulk crystals are filtered, washed with deionized water and dried at room temperature (67.78 % yield based on W). Elemental analysis calcd (%) for $C_{36}H_{32}CuN_{12}O_{42}W_{12}Zn$: C, 11.88; H, 0.89; N, 4.62; found C, 11.78; H, 0.92; N, 4.68. IR (KBr pellets, ν/cm^{-1}): 3440 (m), 3103 (m), 2360 (w), 1611 (m), 1534 (w), 1491 (w), 1417 (w), 1221 (w), 1075 (w), 930 (s), 874 (s), 757 (s), 575 (w), 452 (m).

1.4 Single-Crystal Structure Determination

Single-crystal XRD data of compounds **1, 2** were collected on a Bruker D8 Venture diffractometer with Mo-K$_\alpha$ radiation ($\lambda = 0.71073$ Å) at room temperature. The structure was solved by direct methods, using Fourier techniques, and refined on F^2 by a full-matrix least-squares method. All calculations were carried out with the SHELXTL[2] program.

1.5 Fabrication of 1/2-based TENG

PVDF solution was prepared according to the previous literature method.[3] The prepared PVDF solution was spin-coated on Kapton film and passed through KW-4A desktop leveler at 3000 r min^{-1} for 90 s. Then Cu tape was attached to the other side of Kapton film, and Cu wire was fixed on the Cu tape with conductive silver epoxy. The bulk crystals **1** or **2** were ground mechanically and the crushed crystal is coated on the Cu tape. Then the Cu wire was fixed on the other side of the copper band through the silver epoxy. Using vertical contact separation method, PVDF and crystal powder were contacted face to face as the basic friction layer, and the effective contact area was 25 cm^2. Cu and Kapton were used as the conductive and transitional layers, respectively.

1.6 Materials characterization

Fourier-transform infrared (FT-IR) spectroscopy were measured on potassium bromide (KBr) pellets using a Thermo Nicolet NEXUS 470 FT-IR spectrometer in the region of 4000-400 cm^{-1}. Powder X-ray diffraction patterns (PXRD) were obtained by using a Bruker D8 Advance X-ray powder diffractometer

with Cu-Kα irradiation (λ = 1.54178 Å). The C, H, and N contents were determined by the FLASH EA 1112 elemental analyzer. X-ray photoelectron spectroscopy (XPS) spectra were measured by a Thermo Scientific K-Alpha X-ray photoelectron spectroscopy with Al-Kα X-rays source. The morphologies, sizes and elemental composition of the grinded crystal powder samples were characterized by a Zeiss Merlin Compact field emission scanning electron microscope (FE-SEM) equipped with an energy-dispersive X-ray spectroscopy (EDX) system. The dielectric constants of the tablets were measured by an impedance analyzer (Agilent 4294A) over the frequency range of 10^3 to 10^7 Hz at room temperature. The surface morphologies of the hybrid films were measured by atomic force microscopy (AFM) on the Bruker Dimension Icon. The short circuit current (I_{sc}) was tested by a SR570 low-noise current amplifier (Stanford Research System) and the output voltage (V_o) was tested by 2657A HIGH POWER SYSTEM SourceMeter. The charging curves of 0.22, 1 and 2.2 μF commercial capacitors were obtained by electrochemical workstation (Zennium-Pro 43138). The discharing curves for all commercial capacitors and the charge-discharge profile of the 100 μF capacitor were monitored by CHI660E B18411A.

2. Figures and Tables
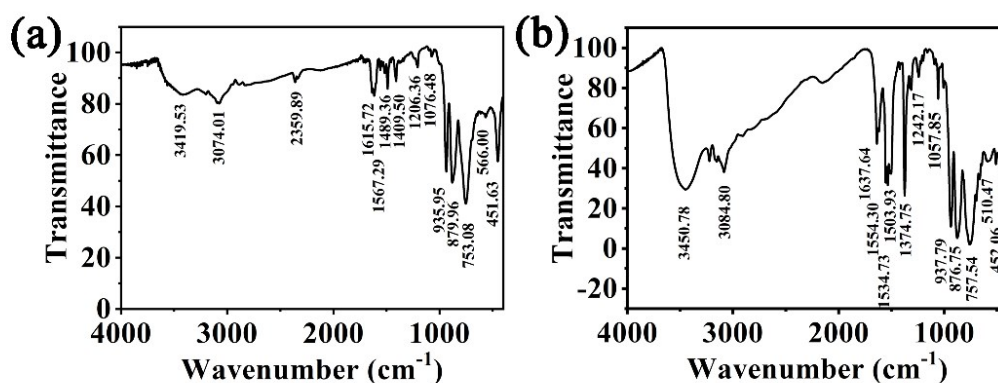
Figure S1. FT-IR spectra of (a) compounds **1** and (b) **2**.
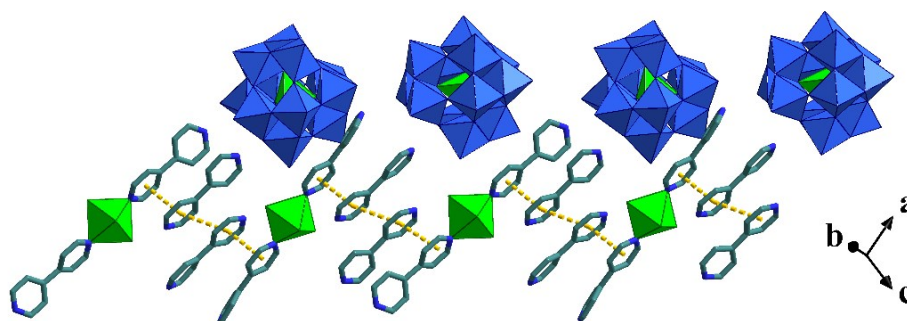
Figure S2. 1D supramolecular network of **1**. Free solvent molecules and hydrogen atoms were omitted for clarity. Color code: WO_6, light blue octahedra; ZnO_4, bright green tetrahedra; ZnN_2O_4 bright green octahedra; C, grey; N, blue.
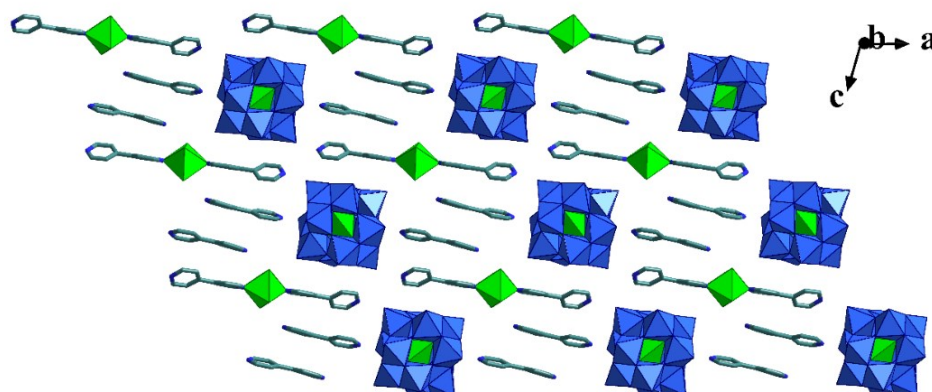
Figure S3. 2D supramolecular network of **1**. Solvent molecules and hydrogen atoms were omitted for clarity. Color code: WO_6, light blue octahedra; ZnO_4, bright green tetrahedra; ZnN_2O_4 bright green octahedra; C, grey; N, blue.
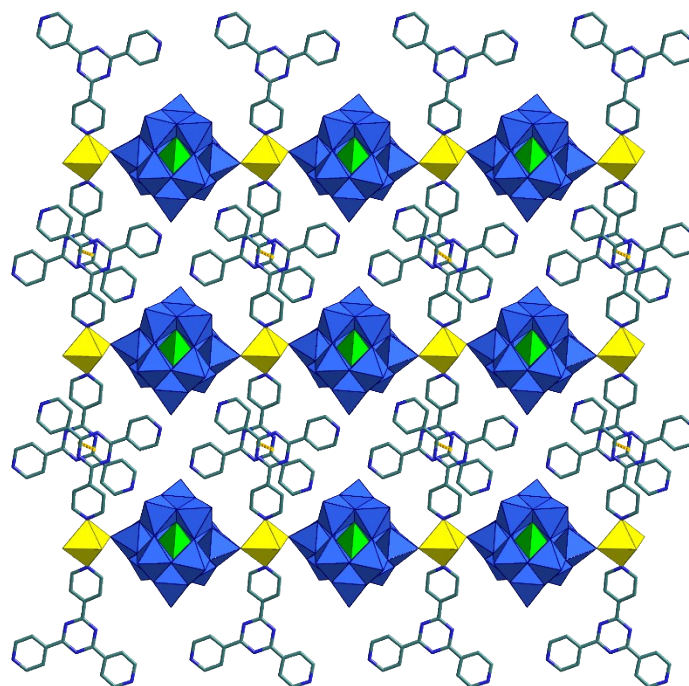
Figure S4. The 2D supramolecular network of **2**. Color code: WO_6, light blue octahedra; ZnO_4, bright green tetrahedra; CuN_2O_4, yellow octahedra; C, grey; N, blue. Hydrogen atoms and free solvent molecules are omitted for clarity.
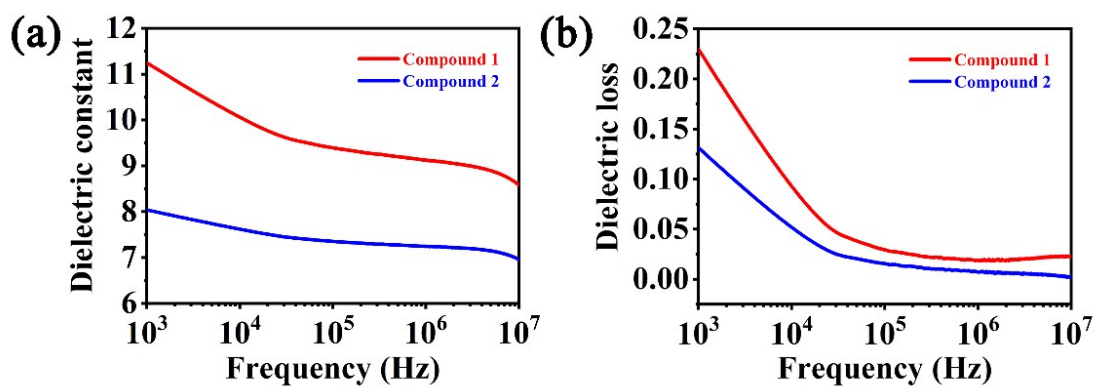
Figure S5. Frequency dependence of (a) dielectric constant and (b) dielectric loss for compound **1** and compound **2**.
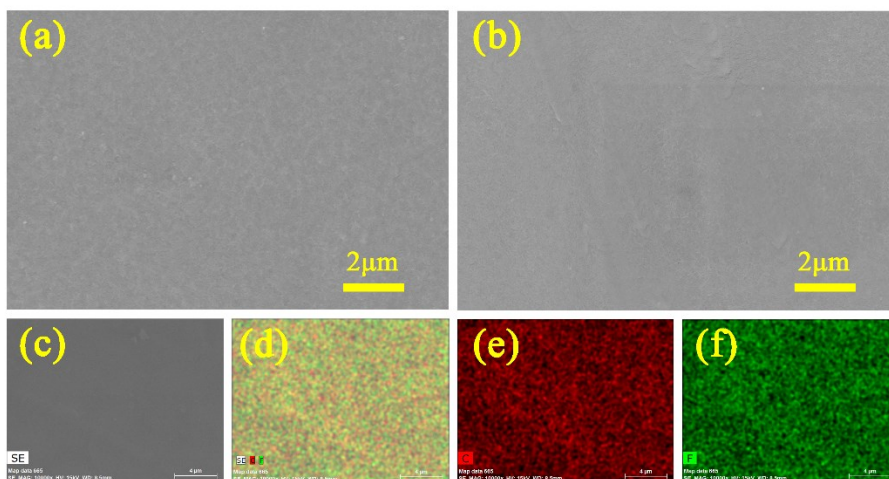
Figure S6. FE-SEM image of PVDF-based friction layer (a) before and (b) after testing. (c-f) EDS mapping analysis of C and F in PVDF.
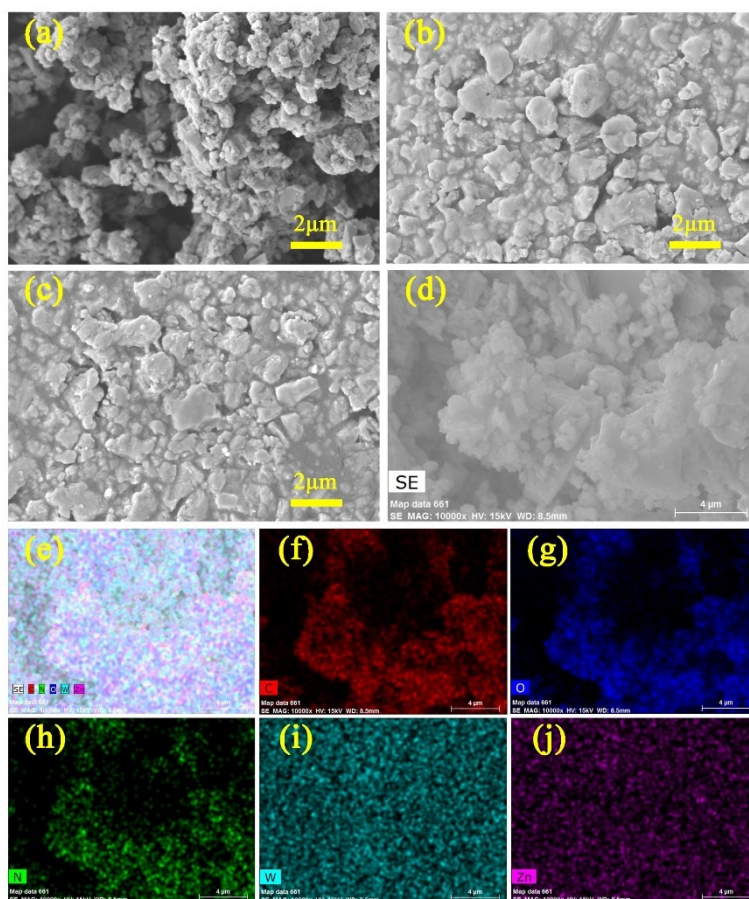
Figure S7. FE-SEM image of (a) ground powder of compound **1**, compound **1**-based friction layer (b) before and (c) after testing. (d-j) EDS mapping analysis of C, O, N, W and Zn in compound **1**.
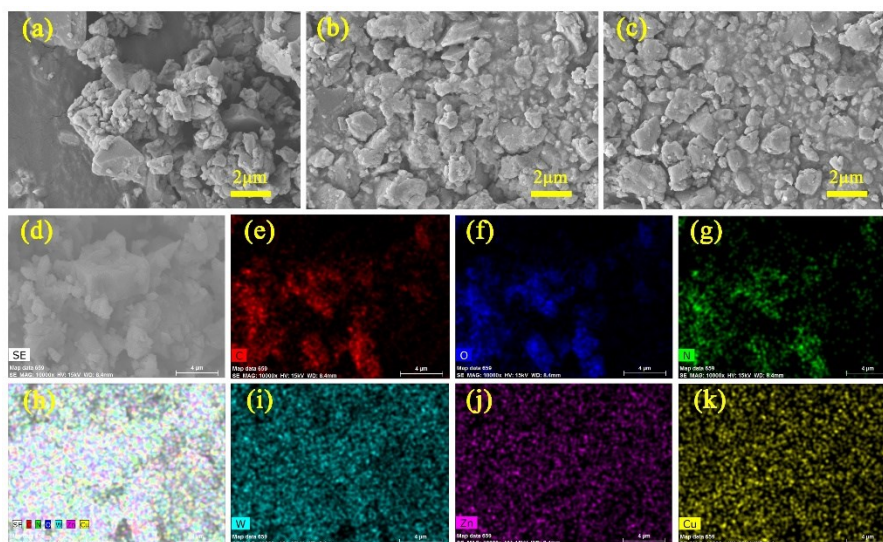
Figure S8. FE-SEM image of (a) ground powder of compound **2**, compound **2**-based friction layer (b) before and (c) after testing. (d-k) EDX mapping analysis of C, O, N, W, Zn and Cu in compound **2**.
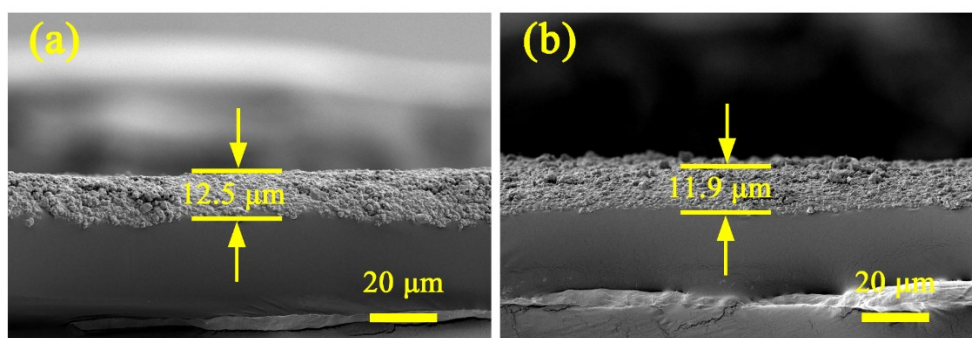
Figure S9. Cross-sectional SEM images of films (a) **1** and (b) **2** on the Cu layer.
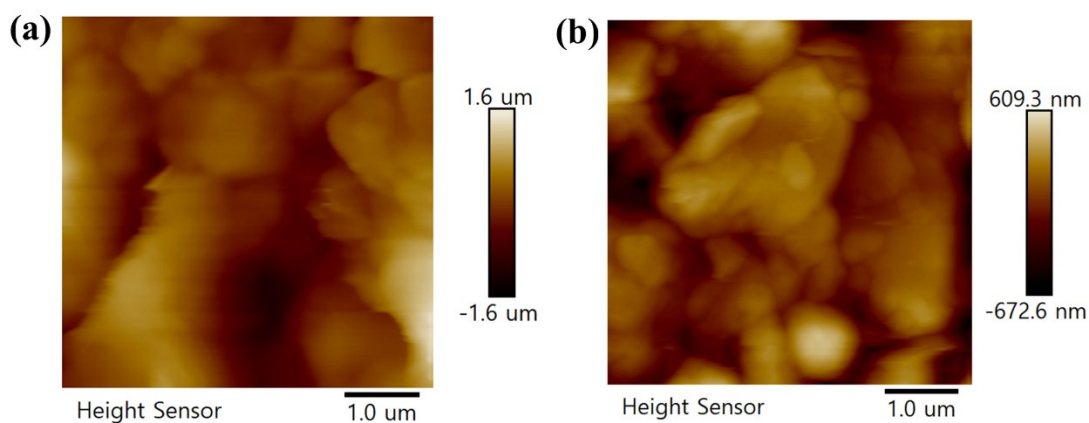
Figure S10. The AFM images of the powder samples (a) **1** and (b) **2** on the electrode (Cu layer). The roughness average (R_a) values: 124 for **1** and 141 nm for **2**.
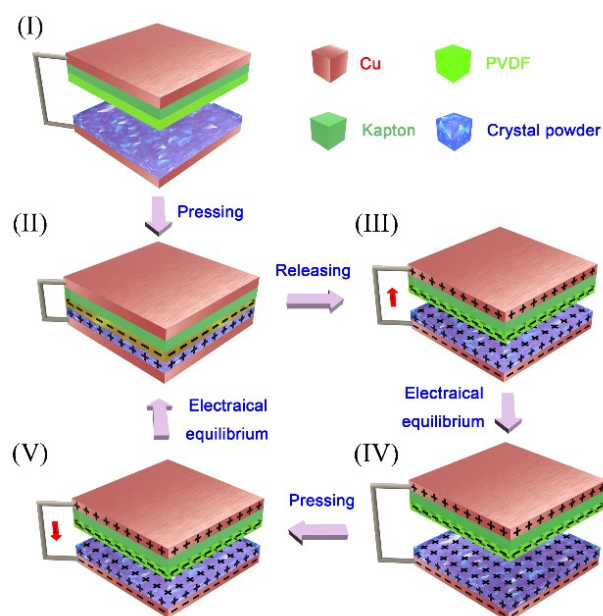
Figure S11. Schematic diagram of working principle for TENG based on compounds **1** and **2** in vertical contact-separation mode.
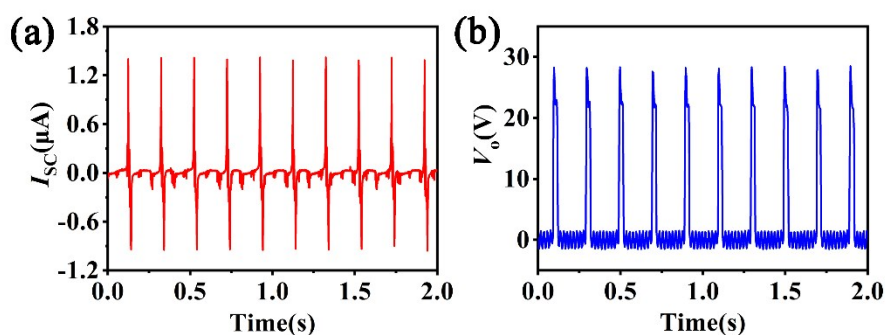
Figure S12. (a) I_{SC} versus time and (b) V_O versus time, of TENG based on compound $(H_2NMe_2)_5H[ZnW_{12}O_{40}]\cdot3.5H_2O$.
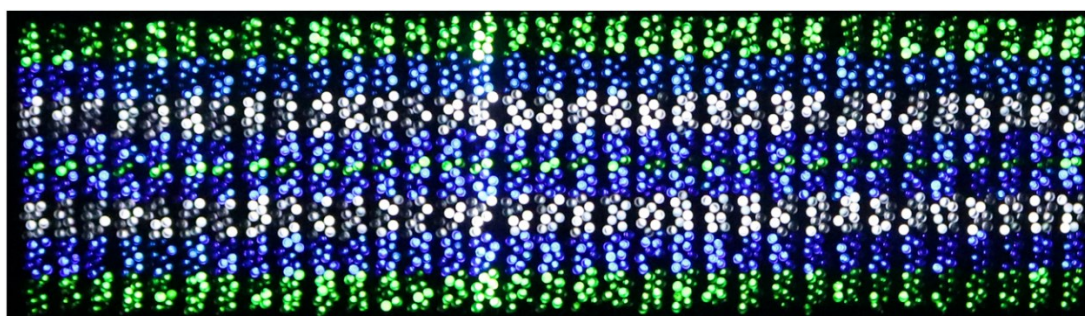
Figure S13. The photograph exhibits that 2046 commercial color LED lights are lit by the TENG based on the compound **1** at the frequency of 8 Hz.
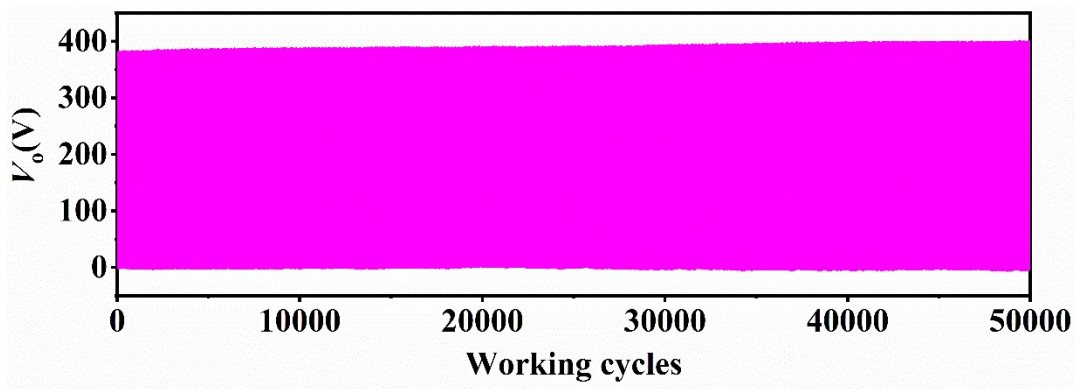
Figure S14. V_o of **1**-based TENG after working 50,000 cycles.

Table S1. Crystallographic data and structure refinement parameters for complexes **1** and **2**.

Complex	1	2
empirical formula	$C_{40}H_{52}N_8O_{48}W_{12}Zn_2$	$C_{36}H_{25}CuN_{12}O_{42}W_{12}Zn$
Mr	3749.83	3632.79
crystal size [mm³]	0.12 × 0.11 × 0.10	0.13 × 0.11 × 0.10
crystal system	monoclinic	monoclinic
space group	$C\,2/c$	Pn
a [Å]	21.2513(7)	14.296(6)
b [Å]	15.2436(5)	15.241(6)
c [Å]	24.1678(8)	16.158(7)
α [°]	90	90
β [°]	106.3880(10)	99.738(14)
γ [°]	90	90
V [Å³]	7511.0(4)	3470(2)
Z	4	2
ρ_{calc} (g cm⁻³)	3.316	3.477
μ (Cu$_{K\alpha}$) [mm⁻¹]	19.019	20.534
$F(000)$	6720.0	3216.0
θ range [°]	2.81 to 27.48	2.477 to 25.026
limiting indices	-25 ≤ h ≤ 25	-17 ≤ h ≤ 17
	-18 ≤ k ≤ 18	-18 ≤ k ≤ 18
	-28 ≤ l ≤ 28	-19 ≤ l ≤ 19
collected reflns	79607	54164
unique reflns	6630	12199
absorption correction	multi-scan	multi-scan
max./min. transmission	0.736/1.000	0.7961/1.000
data/restraints/parameters	6630/0/533	12199/219/918
goodness of fit	1.267	1.038
R_1/wR_2 [I >2σ(I)][a]	0.0293/ 0.0695	0.0366/0.0815
R_1/wR_2 (all data)[a]	0.0299/0.0698	0.0410/0.0844
CCDC	2048936	2048937

[a] $R_1=\Sigma\|F_0\|-\|F_c\|\|$ (based on reflections with $F_0^2>2\sigma F^2$). $wR_2=[\Sigma[w(F_0^2-F_c^2)^2]/\Sigma[w(F_0^2)^2]]^{1/2}$; w=1/[σ²($F_0^2$)+(0.095$P$)²]; $P=[\max(F_0^2, 0)+2F_c^2]/3$(also with $F_0^2>2\sigma F^2$)

3. References

1 A. V. Anyushin, P. A. Abramov, A. L. Gushchin, C. Vincent and M. N. Sokolov, *Russ. J. Inorg. Chem.*, 2017, **62**, 397-403.

2 a) G. M. Sheldrick, *Acta Cryst.*, 2015, **A71**, 3-8; b) G. M. Sheldrick, *Acta Cryst.*, 2015, **C71**, 3-8.

3 a) S. Cui, Y. Zheng, J. Liang and D. Wang, *Nano Res.*, 2018, **11**, 1873-1882; b) Z. Wang, L. Cheng, Y. Zheng, Y. Qin and Z. L. Wang, *Nano Energy*, 2014, **10**, 37-43.